Protein Science (1999), *8*:1023–1031. Cambridge University Press. Printed in the USA.

Ternary complex structure of human HGPRTase, PRPP, Mg^{2+}, and the inhibitor HPP reveals the involvement of the flexible loop in substrate binding

GANESARATNAM K. BALENDIRAN,[1] JOSÉ A. MOLINA,[2,6] YIMING XU,[3,7] JAN TORRES-MARTINEZ,[4] ROBERT STEVENS,[5] PAMELA J. FOCIA,[4] ANN E. EAKIN,[4] JAMES C. SACCHETTINI,[1] AND SYDNEY P. CRAIG III[4]

[1]Department of Biochemistry and Biophysics, Texas A&M University, College Station, Texas 77843-2128
[2]Department of Biochemistry, University of Puerto Rico–Medical Sciences Campus, San Juan, Puerto Rico 00936
[3]Department of Biochemistry, Temple University School of Medicine, Philadelphia, Pennsylvania 19140
[4]Laboratory of Molecular Parasitology and Drug Design, School of Pharmacy, CB#7360, University of North Carolina at Chapel Hill, Chapel Hill, North Carolina 27599
[5]Mass Spectrometry Facility, Section of Biochemical Genetics, Duke University Medical Center, Research Triangle Park, North Carolina 27709

(RECEIVED December 1, 1998; ACCEPTED February 18, 1999)

Abstract

Site-directed mutagenesis was used to replace Lys68 of the human hypoxanthine phosphoribosyltransferase (HGPRTase) with alanine to exploit this less reactive form of the enzyme to gain additional insights into the structure activity relationship of HGPRTase. Although this substitution resulted in only a minimal (one- to threefold) increase in the K_m values for binding pyrophosphate or phosphoribosylpyrophosphate, the catalytic efficiencies (k_{cat}/K_m) of the forward and reverse reactions were more severely reduced (6- to 30-fold), and the mutant enzyme showed positive cooperativity in binding of α-D-5-phosphoribosyl-1-pyrophosphate (PRPP) and nucleotide. The K68A form of the human HGPRTase was cocrystallized with 7-hydroxy [4,3-d] pyrazolo pyrimidine (HPP) and Mg PRPP, and the refined structure reported. The PRPP molecule built into the $[(F_o - F_c)\phi_{calc}]$ electron density shows atomic interactions between the Mg PRPP and enzyme residues in the pyrophosphate binding domain as well as in a long flexible loop (residues Leu101 to Gly111) that closes over the active site. Loop closure reveals the functional roles for the conserved SY dipeptide of the loop as well as the molecular basis for one form of gouty arthritis (S103R). In addition, the closed loop conformation provides structural information relevant to the mechanism of catalysis in human HGPRTase.

Keywords: birth defects; inhibitor design; PRPP; PRTase; purine analog; rapid quench experiments; steady-state kinetic studies

Hypoxanthine phosphoribosyltransferase [HGPRTase; EC 2.4.2.8; hypoxanthine pyrophosphate phosphoribosyltransferase] is a purine salvage enzyme that catalyzes the reversible transfer of the 5-phosphoribosyl group between α-D-5-phosphoribosyl-1-pyrophosphate (PRPP) and a purine base (hypoxanthine or guanine) to form a purine nucleotide [inosine monophosphate (IMP) or guanosine monophosphate (GMP)]. HGPRTase has been extensively investigated because defects within the human enzyme are associated with genetically inherited gouty arthritis and Lesch–Nyhan syndrome (Lesch & Nyhan, 1964; Seegmiller et al., 1967; Kelley et al., 1969). In addition, many parasites have lost the ability to synthesize purines de novo and are forced to rely upon salvage pathways for the purines needed in cellular metabolism (Berens et al., 1995); therefore, enzymes in these pathways have been proposed as potential targets for drugs in the chemotherapeutic treatment of a number of diseases caused by parasites (Musick, 1981).

For those HGPRTases that have been studied kinetically, the enzyme-catalyzed reaction has been shown to proceed via a functionally ordered sequential bi-bi mechanism in which PRPP binds first to the enzyme followed by a purine base (Giacomello &

Reprint requests to: G.K. Balendiran, Department of Biochemistry and Biophysics, Texas A&M University, College Station, Texas 77843-2128; e-mail: balendra@reddrum.tamu.edu.
[6]Present address: University of Puerto Rico, Cayey, Puerto Rico 00736.
[7]Present address: Department of Biochemistry, Albert Einstein College of Medicine, Bronx, New York 10461.

Abbreviations: A, adenine; C, cytosine; dNTP, deoxynucleotide triphosphate; DTT, dithiothreitol; G, guanine; GMP, guanosine 5′-monophosphate; HGPRTase, hypoxanthine phosphoribosyltransferase; HPP, 7-hydroxy [4,3-d] pyrazolo pyrimidine; Hx, hypoxanthine; IMP, inosine 5′-monophosphate; ncs, noncrystallographic symmetry; OPRTase, orotate phosphoribosyltransferase; PCR, polymerase chain reaction; PPi, inorganic pyrophosphate; PRPP, α-D-5-phosphoribosyl-1-pyrophosphate; SDS, sodium dodecyl sulfate; T, thymine; U, uracil.

Salerno, 1978; Yuan et al., 1992; Xu et al., 1997; Munagala et al., 1998). Release of products is also functionally ordered with inorganic pyrophosphate (PPi) leaving first, followed by the nucleoside monophosphate. Kinetic studies showed that PRPP and nucleoside monophosphates bind competitively to the apo form of the enzyme. In contrast, only minimal values for the K_d have been determined for the weak binding of purine bases or PPi to the free form of HGPRTase, although it was shown that these two substrates bind cooperatively to form a dead end complex with the enzyme (Xu et al., 1997).

The solution of the three-dimensional structure for the human HGPRTase (Eads et al., 1994) permitted us to deduce the structural and biochemical roles of amino acids in the enzyme catalyzed reaction as well as to interpret the molecular basis for a number of naturally occurring mutations that are associated with several debilitating conditions. An unresolved question has been the identity of enzyme residues that form interactions with the PPi moiety of PRPP or with PPi itself. These residues may donate a proton to a leaving PPi in the forward direction, although the moderately basic pK_a (9.1) of that group (Dawson et al., 1986) suggests that enzymic protonation will not be required to provide stabilization. Based on a positional similarity to Lys73 of orotate phosphoribosyltransferase (OPRTase), in both the primary and tertiary structures, Lys68 was proposed to provide catalytic assistance by binding pyrophosphate in the human HGPRTase (Eads et al., 1994; Scapin et al., 1994). In OPRTase, mutagenesis of Lys73 to alanine resulted in a 50-fold decrease in k_{cat} and 100-fold decrease in catalytic efficiency (Ozturk et al., 1995).

Recent crystal structures of the HGPRTase of *Trypanosoma cruzi* (Focia et al., 1998a, 1998b) provide new evidence for the possible role for Lys68. In the trypanosomal enzyme, Lys68 interacts with pyrophosphate atoms of PRPP (as originally proposed by Eads et al., 1994), but via hydrogen bonds involving main-chain rather than side-chain atoms. Also, the NZ-amine of Lys68 in the trypanosomal enzyme interacts with residues belonging to the opposing subunit of the dimer, possibly providing a mechanism for allosteric interactions between subunits. At the time the present study was initiated, the K68A mutant form of the human enzyme was created as part of a strategy to solve the structure of the human enzyme in a closed conformation with substrates bound. Subsequent analyses of the kinetic properties of the K68A mutant indicated that the activity was too high for this strategy to succeed. However, the kinetics described herein provide the first evidence in HGPRTase for positive cooperativity between subunits in the binding of substrates. The structure of the K68A mutant form of human enzyme does not allow detailed interpretations for interactions involving the side-chain atoms of Lys68, but the structural basis for the observed cooperativity can be interpreted in the context of the proposed role for the homologous residue in a related HGPRTase (Focia et al., 1998a, 1998b).

A structure with the substrates of the forward reaction bound would be useful for understanding structure–function relationships of the human HGPRTase and for designing selective inhibitors targeted to the HGPRTase of pathogens. Strategies for achieving such a structure involved using a nonreactive substrate analog in the crystallization trials and/or an enzyme incapable of completing the enzyme catalyzed chemistry. Thus, the less reactive K68A form of the human HGPRTase was crystallized in the presence of Mg PRPP, and a hypoxanthine analog [7-hydroxy [4,3-d] pyrazolo pyrimidine (7-deaza-8-aza-hypoxanthine, HPP)]. The X-ray structure generated from these crystals reveals the atomic interactions between HPP and Mg PRPP in the active site of human HGPRTase and the role of the long flexible loop predicted to close over the active site during the reaction (Eads et al., 1994).

Results and discussion

Cocrystallization of HPP and Mg PRPP with the human HGPRTase

The nonreactive hypoxanthine analog, HPP, formerly has been shown to bind competitively (with an apparent K_i of 31.5 ± 0.5 μM) to the active site of the human HGPRTase (Eakin et al., 1997). The K68A form of the human enzyme was crystallized in the presence of both HPP and Mg PRPP. The resulting structure revealed the presence of the ligands HPP and Mg PRPP (Figs. 1, 2) in the active sites of both the molecules (subunits A and B) of the dimer.

Overall structure

Crystals of the K68A HGPRTase HPP PRPP complex were isomorphous with crystals of the human HGPRTase GMP complex used to determine the HGPRTase structure. There was a dimer of the enzyme in the asymmetric unit with the RMS difference for the Cα atoms of 1.3 Å between the subunits A and B, including residues Leu101 to Gly111 of the flexible active site loop and 1.3 Å excluding the flexible loop. The catalytic core of the enzyme, consisting of 120 residues out of 217, resembles a dinucleotide

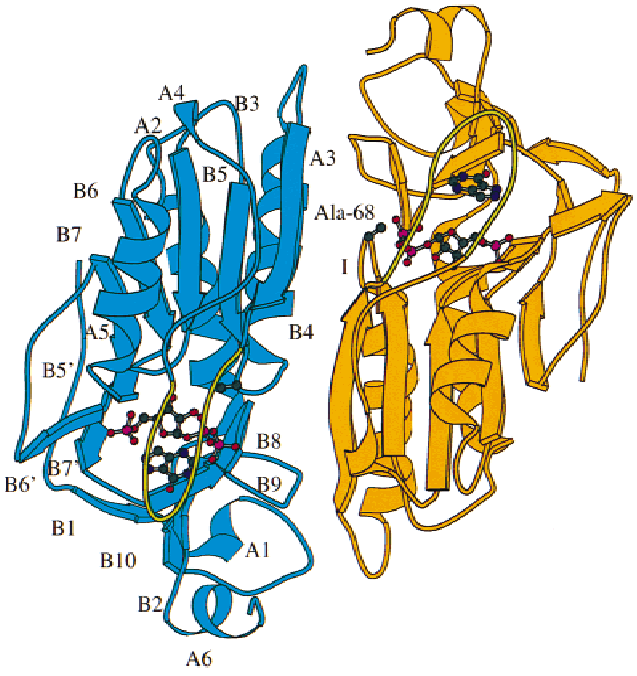

Fig. 1. Structure of human HGPRTase Mg PRPP HPP complex, where HPP, PRPP, and the side-chain atom of residue Ala68 are shown in ball-and-stick representation. The dimers that forms the asymmetric unit with both the molecules in the closed loop conformation are referred to as subunit A (cyan) and B (brown). The flexible loop in the closed conformation is shown in greenish yellow. Program Molscript was used to create the figure (Kraulis, 1991).

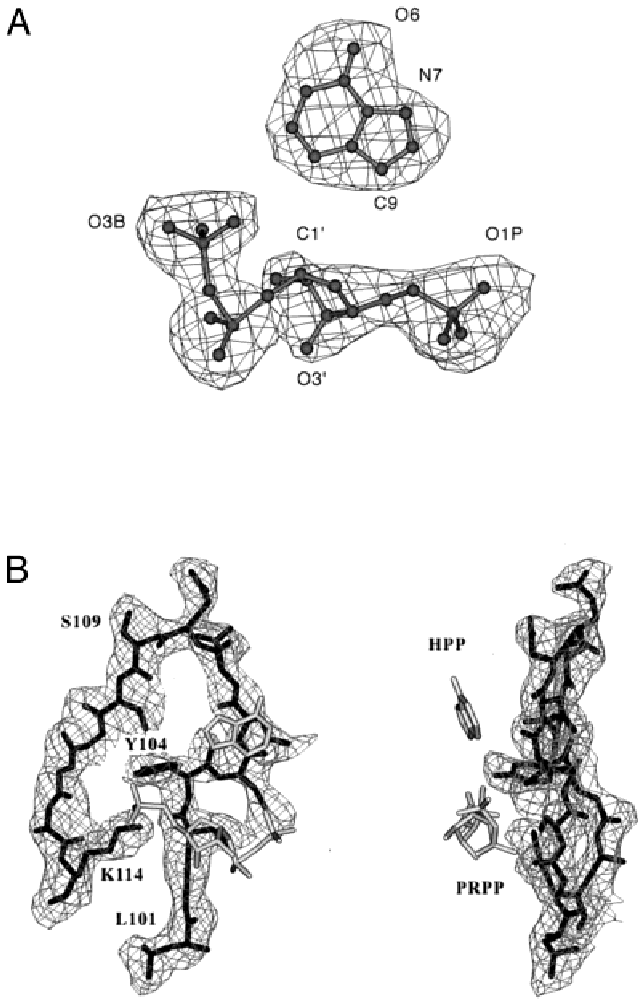

Fig. 2. A: Electron density maps calculated with $[(F_o - F_c)\phi_{calc}]$ coefficients (contoured at 1.8σ). Areas displayed correspond to HPP and PRPP moieties. **B:** Front and side views of the long flexible loop electron density calculated with $[(F_o - F_c)\phi_{calc}]$ coefficients (contoured at 1.4σ). Relative orientation of HPP and PRPP is shown without density. This figure was created using the program SETOR (Evans, 1993).

binding fold that contains a region of a twisted parallel β-sheet of five β-strands (B3, B4, B5, B6, and B7) surrounded by four α-helices (A2, A3, A4, and A5) (Fig. 1). The difference Fourier electron density maps calculated with $[(F_o - F_c)\phi_{calc}]$ coefficients showed interpretable density for HPP and PRPP in the cleft located above the central β-sheet of the core (Fig. 2A). In the Mg PRPP HPP complex, the two molecules that form the asymmetric unit have interpretable density for the main-chain and most of the side-chain atoms of the long flexible loop in addition to the density for the ligands in their active sites (Fig. 2B).

HPP binding

HPP was bound in the active site cavity formed by a combination of hydrogen bonds and van der Waals interactions between HPP and residues Val187, Lys165, Asp137, Phe186, Leu192, and Ile135. The stacking interaction between HPP and Phe186 is similar to that observed between the guanine of GMP and Phe186 in the GMP complex. However, there are differences in hydrogen bonds (interatomic distance $<$3.2 Å used for the selection) of HPP and GMP in the active site of the human HGPRTase. In this regard, hydrogen bonds are observed between the N7 and N8 of the purine analog HPP and the side-chain atoms of Lys165 and Asp137, respectively (Fig. 3). These hydrogen bonds were not observed when GMP was bound to the active site of the enzyme (Eads et al., 1994). In the GMP complex, a hydrogen bond was observed between the O6 of GMP and NZ of Lys165, whereas in HPP PRPP complex the O6 of HPP forms a hydrogen bond with the main-chain N atom of Val187 and Lys165 now forms a hydrogen bond with the N7 of HPP (Fig. 3). The absence of the hydrogen bond between the side-chain NZ atom of Lys165 and O6 of HPP is in good agreement with the findings reported in the *Escherichia coli* XGPRTase structure. The Lys115 in *E. coli* XGPRTase, which corresponds to the Lys165 in human HGPRTase, was found to adopt a conformation in which the terminal NZ group of Lys115 is longer than hydrogen bonding distance from the O6 of the guanine base (Vos et al., 1998). The hydrogen bonds that were observed between the N2 of GMP and the main-chain O atoms of Val187 and Asp193 are no longer observed in the structures with HPP, which possesses a hydrogen atom instead of an amino group at this position. The difference in the pattern of hydrogen bonds for HPP and the guanine moiety of GMP causes a shift in the position of the purine rings in the active site of the enzyme. The hydrogen bonds seen between HPP and the active site residues help to position atom 9 of the purine base in close proximity to the ribose moiety where an in-line nucleophilic attack at C1′ by the lone-pair electrons of N9 would have the best geometric arrangement. Positioning PRPP in this density resulted in an ~5 Å distance between the C9 of HPP and C1′ of PRPP. Subtle differences in details of the binding of HPP to the human and a trypanosomal HGPRTase may be significant and could be relevant for the design of compounds that would selectively inhibit the *T. cruzi* enzyme.

Mg PRPP binding

The most noticeable feature at the primary sequence level of the Type I PRTase family is a conserved PRPP binding motif (Wilson et al., 1983; Hove-Jensen et al., 1986), formed by residues Val129 through Lys140 in human HGPRTase, which is located between helices A4 and A5. The PRPP bound in the active site is surrounded by residues Leu67, Ala68, Gly69, Lys102, Ser103, Tyr104, Lys114, Glu133, Asp134, Thr138, Gly139, Thr141, and Asp193 (Fig. 3). Phosphate binding loop residues Thr138, Gly139, Lys140, and Thr141 of the PRPP binding motif form hydrogen bonds with the 5′ phosphate of PRPP. Conserved acidic residues Glu133 and Asp134 were found to form hydrogen bonds directly with O3′ and O2′, respectively. Divalent metal ion Mg^{2+}, required for PRPP binding and catalysis (Musick, 1981; Bhatia et al., 1990), was found to be coordinated in octahedral geometry with O3′, O2′, one of the oxygen atoms of the pyrophosphate moiety (O2A), O1′ of PRPP, and two water molecules.

Flexible loop

Interactions with the bound Mg PRPP molecule show the role of the flexible loop in human HGPRTase. In the GMP complex, a flexible loop defined by residues Leu101 to Gly111 of subunit B has poor electron density and is observed in a “loop open” conformation. The human HGPRTase Mg PRPP HPP complex structure shows that after Mg PRPP and HPP are bound, flexibility

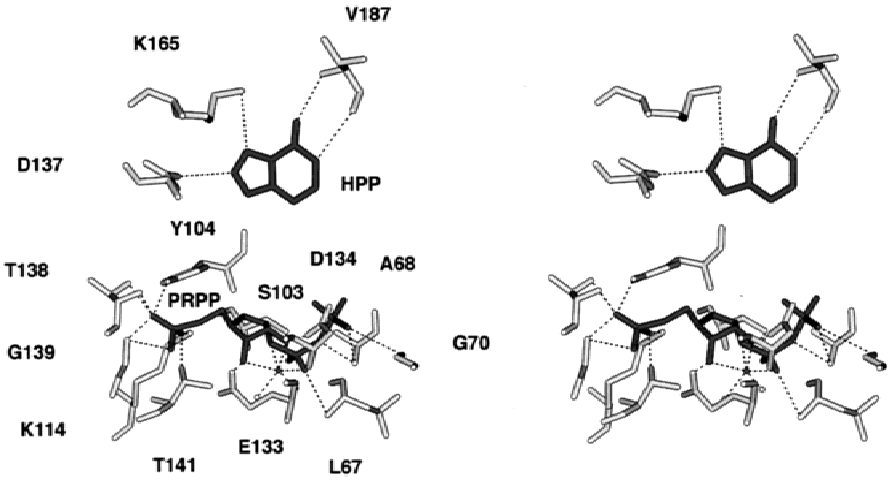

Fig. 3. Hydrogen bonds between HPP and active site residues N8···OD2 D137, N7···NZ K165, O6···N V187, and N1···O V187; Mg PRPP and active site residues O2′···OD1 D134, O3′···OE2 E133, O1A···OG S103, O3A···N A68, O2B···N G70, O1B···N A68, O2A···N L67, O3B···N A68, O1P···OH Y104, O1P···OG1 T138, O1P···N G139, O1P···N T138, O2P···N G139, O3P···NZ K114, O3P···OG1 T141, Mg···O3′, Mg···O2′, Mg···O2A, Mg···O1′, Mg···O H_2O, Mg···O H_2O are shown in stereo.

becomes restricted, and the corresponding loop accommodates a new conformation ("loop closed") in both subunits A and B.

The structural rearrangements made by residue Tyr104 in the closed-loop conformation allow this residue to form interactions with the 5′ phosphate moiety of PRPP, which positions the side chain over the O4′ atom of the ribose moiety (Figs. 2, 3). Also, the α-helix (A4), formed by residues 116 to 123 in the presence of GMP, is shifted in the presence of Mg PRPP, which brings residues 100 to 115 of the closed loop closer to the active site than in the open-loop conformation. This shift may facilitate the flexible loop attaining the closed conformation. Hence, this feature may play an important role in binding Mg PRPP and protecting an oxocarbonium ion-like intermediate from hydrolysis by the bulk solvent if the reaction indeed goes through proposed S_N1-type nucleophilic displacement catalytic mechanism.

In the presence of Mg PRPP, the side chain of Ser103 forms a hydrogen bond with the O1A atom of pyrophosphate (Fig. 3). This orientation is a bit surprising in the context of kinetic studies of a mutant form (S103R) of the human HGPRTase resulting in Gout ($HGPRTase_{Munich}$) (Wilson et al., 1983). For this mutant, the Michaelis constant for binding hypoxanthine was 100-fold above that for the wild-type enzyme, while that for PRPP was unaffected. Also, the interactions involving the side chain of Ser103 differ with those observed for Ser103 in a closed conformation of the *T. cruzi* HGPRTase with HPP and PRPP bound in the active site (Focia et al., 1998a). In the trypanosomal HPRTase structure, the amide nitrogen of Ser103 was modeled within hydrogen bonding distance of the O1A atom of pyrophosphate and the side chain was participating in hydrogen bonds that could be essential for proper positioning and closure of the flexible loop. In both the human and trypanosomal HGPRTases, the substitution of arginine at this position would be expected to interfere with the loop closure and the binding of substrates.

Ser109 in the human HGPRTase PRPP complex forms hydrogen bonds with the side-chain atoms of Gln151 of the symmetry related molecule. The substitution of Leu for Ser at position 109 would disrupt the hydrogen bond that may be important in stabilizing the closed-loop conformation in the presence of PRPP. Thus, the Mg PRPP complex structure of the human HGPRTase indicates that the serine at position 109 is necessary for adopting the closed-loop conformation required for the normal function of human HGPRTase, and explains why the S109L mutant form of the human HGPRTase has altered Michaelis constants (an increased K_m for hypoxanthine but a normal K_m for PRPP), which result in gouty arthritis (Wilson et al., 1983). In addition, Ser109 may be one of the residues at the tetramer interface involved in interactions with the symmetry-related molecule and playing an important role for the formation of the tetramer. It has been shown under physiological conditions that the human HGPRTase is active as a tetramer (Strauss et al., 1978).

Role of residue 68 in active site loop I of the HGPRTase

Information relevant to the role of Lys68 in the human enzyme may be provided by the 1.4 Å structure for the *T. cruzi* HGPRTase (Focia et al., 1998b), with interpretable electron density for the amino acid that is homologous with Lys68 in the human enzyme. In the trypanosomal enzyme, the side chain is oriented away from the active site and forms a hydrogen bond with a main-chain oxygen belonging to a residue in the second subunit in the dimer of the enzyme. It was suggested that this provides a mechanism for communication between the active sites of the subunits in the dimer (Focia et al., 1998b). Furthermore, the peptide bond between Leu67 and Lys68 in the trypanosomal enzyme is in an unusual *cis* conformation, exposing the carbonyl of Leu67 and the amide nitrogen of Lys68 to the active site. The residues flanking Lys68 (Leu67 and Gly69) are among the 13 most highly conserved residues in HGPRTases and, in addition to other factors, their presence could possibly favor the formation of the *cis* peptide bond between the residues at position 67 and 68. Nonproline *cis* peptides are rarely observed in crystal structures and have been identified with confidence only in those structures solved at relatively high resolution. In addition to the trypanosomal enzyme, *cis* peptides have been observed in the analogous active site loop I in *Tritrichomonas foetus* HGXPRTase (Somoza et al., 1996), the *E. coli* XPRTase (Vos et al., 1997), the *E. coli* OPRTase (Henriksen et al., 1996), and *E. coli* glutamine phosphoribosylpyrophosphate amidotransferase (Krahn et al., 1997). The structure of human

HGPRTase at a moderate resolution does not allow the unambiguous assignment of the *cis* peptide in the active site loop, and the peptide bond at position 68 is not classified as *cis* conformation (Laskowski et al., 1993) even though the loop formed by residues 67, 68, and 69 form a sharp turn. However, the density observed in the human HPP PRPP complex structure indicates that main-chain atoms of Ala68 form hydrogen bonding and van der Waals interactions with the pyrophosphate moiety of PRPP. Thus, the kinetic data reported here, indicating that the substitution of alanine for lysine at position 68 affects the rate constants for steps in catalysis subsequent to the chemical step, could be due to an alteration in a mechanism affecting interactions between residues in this loop and substrates or products in the active site.

Comparison of human and T. cruzi HGPRTase HPP PRPP complexes

Human and *T. cruzi* HGPRTases share 33% sequence identity. Even though Lys68 varies among this class of enzymes, Ser103, Tyr104, Glu133, Asp134, Asp193, and Arg199 are several invariant residues among them. The structure of the HGPRTase of *T. cruzi*, with HPP and PRPP bound in the active site, revealed the presence of a second Mg ion forming coordinated interactions with oxygens of both the α and β phosphate moieties of PRPP, as well as interactions with the side chain of the conserved Asp193 (Focia et al., 1998a). In addition, a water molecule, coordinated by this Mg ion, formed a hydrogen bond with the nitrogen at the position 3 of the purine base. Thus, interference with these interactions by the substitution of asparagine at position 193 would be expected to affect the Michaelis constants for both PRPP and purine substrates. A similar ion in the structure of the human HGPRTase would provide a molecular explanation for the D193N mutation. However, the resolution of our structure does not allow us to conclude the existence of a second Mg ion, which is coordinated to Asp193 in the current structure, and a second Mg ion has not been observed in other PRTase structures with PRPP in their active sites (Scapin et al., 1995; Krahn et al., 1997; Vos et al., 1998). In addition, the side chain of Lys68 forms a hydrogen bond with an Asp residue of the same subunit in the *T. cruzi* HPP PRPP complex. This residue corresponds to the conserved residue Glu196 in human HGPRTase. However, in the human K68A HGPRTase due to the absence of the side chain (atoms of Lys68), Glu196 is not capable of forming this interaction; instead, it points away from Ala68. Disruption of this interaction may be responsible for the differences seen in the current structure with the residues Asp193 and Arg199. Future studies will resolve this discrepancy and provide evidence to clarify the functional role for the side chain of Asp193. In the human HPP PRPP complex, terminal nitrogens of residue Arg199 form hydrogen bonding interactions with residue Gly70 of the same molecule, while PRPP makes interactions with residues Ala68 and Gly69. Arg199 in the *T. cruzi* HPP PRPP complex interacts with the pyrophosphate moiety of PRPP, as predicted earlier (Craig et al., 1997), and the side chain of residue Asp193.

The RMS differences for Cα atoms between the human and *T. cruzi* HPP PRPP complexes are 1.7 Å (subunit A), 1.5 Å (subunit B), and 2.5 Å (dimer). The largest difference between the human and *T. cruzi* HGPRTase HPP PRPP complexes is due to the flexible loop. In the human complex structure, both molecules in the asymmetric unit adopt the closed loop conformation, but in the trypanosomal structure, one molecule adopts the closed conformation while the other molecule of the asymmetric unit adopts an open conformation that is stabilized by crystal contacts (Focia et al., 1998a). However, differences in the hydrogen bonding pattern for Lys68 are also noted for the trypanosomal HGPRTase in going from the open to closed active sites, and because this side chain is absent in the present mutant structure, the observance of two closed active sites in the human HGPRTase could be a consequence of the substitution of alanine for lysine at position 68. Alternatively the ability to form two closed active sites simultaneously may reflect a true difference in the catalytic mechanisms between the human and parasite HGPRTases and may become important in structure-based inhibitor design.

Kinetic studies of K68A form of human HGPRTase

Based on our earlier crystal structure of human HGPRTase, Lys68 was proposed to have a functional role in binding Mg^{2+}-pyrophosphate (MgPPi) in the HGPRTase catalyzed reaction (Eads et al., 1994). Thus, replacement of Lys68 by alanine would be expected to reduce catalytic activity and increase the equilibrium binding constants for binding both PRPP and PPi. Steady-state kinetic studies of the purified recombinant K68A form of the human HGPRTase were performed at 23 °C (Table 1) using the modified procedures reported earlier (Xu et al., 1997). Compared to the wild-type enzyme, values of k_{cat} in the mutant enzyme were reduced by three- to fivefold, whereas the K_m values were increased by eightfold for hypoxanthine and threefold for PRPP and IMP, but were virtually unchanged for PPi. The combined effect of the changes produced decreases in catalytic efficiency (k_{cat}/K_m) of 8- to 10-fold for IMP, PPi, and PRPP, and 30-fold for hypoxanthine. These results indicate that the substitution of alanine for lysine at position 68 of the human HGPRTase was modestly deleterious for turnover rates and catalytic efficiency.

Previous chemical quench studies of the wild-type HGPRTase revealed that in the forward reaction, steps subsequent to phosphoribosyl transfer chemistry were rate limiting. Although K68A displayed only a modestly reduced k_{cat} in the forward reaction, it was possible that the decrease was due to specific alteration in the rate of the chemical step. To test this hypothesis, the rate constant for the chemical step was directly assessed for K68A by examining its pre-steady-state kinetic behavior. As shown in Figure 4, the time course of pre-steady-state formation consisted of an initial rapid exponential phase followed by a slow linear phase behavior diagnostic of fast chemistry. Furthermore, the results from rapid-quench experiments clearly established that K68A is still able to catalyze rapid phosphoribosyl transfer chemistry. In fact, the observed burst rate (690 s^{-1}) was slightly higher than that for the wild-type (130 s^{-1}; Xu et al., 1997) and was stoichiometric (0.95 mol IMP/mol subunit). Thus, the reduction in k_{cat} for K68A was solely due to change in rate constants for steps subsequent to the chemical step.

Ligand binding experiments were performed to better understand the effects of mutating Lys68. Surprisingly, unlike the wild type, the binding data deviate from the behavior expected from a single class of binding sites. Instead, the data were well fit by a model incorporating positive cooperativity (Scheme 1).

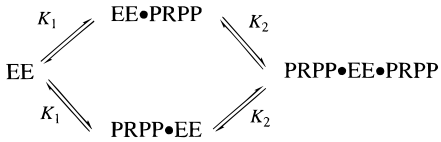

(Scheme 1)

Table 1. *Kinetic parameters at 23 °C*

	Wild-type enzyme	K68A mutant	Ratio (wild-type/mutant)
K_m (Hx)	0.45 μM	3.9 ± 4 μM	0.12
k_{cat}	6.0 s^{-1}	1.7 ± 0.2 s^{-1}	3.5
K_m (PRPP)	31 μM	95 ± 22 μM	0.33
k_{cat}	6.0 s^{-1}	1.9 ± 0.2 s^{-1}	
k_{cat}/K_m (Hx)	1.3×10^7 s^{-1} M^{-1}	4.4×10^5 s^{-1} M^{-1}	30
k_{cat}/K_m (PRPP)	2.1×10^5 s^{-1} M^{-1}	2.0×10^4 s^{-1} M^{-1}	11
K_m (IMP)	5.4 μM	11.4 ± 1.6 μM	0.35
k_{cat}	0.17 s^{-1}	0.037 ± 0.001 μM	4.6
K_m (PPi)	25 μM	30.9 ± 7.2 μM	0.81
k_{cat}	0.17 s^{-1}	0.036 ± 0.003 s^{-1}	
k_{cat}/K_m (IMP)	3.1×10^4 s^{-1} M^{-1}	3.2×10^3 s^{-1} M^{-1}	9.7
k_{cat}/K_m (PPi)	6.8×10^3 s^{-1} M^{-1}	1.2×10^3 s^{-1} M^{-1}	8.2
k_{cat} (forward)/k_{cat} (reverse)	~35-fold	~50-fold	

Similar results were obtained with two sets of independent experiments. In Scheme 1, the dimeric form of the enzyme functions as the independent binding unit. The two subunits were assumed to be identical in the apo-form of the dimer with low affinity for PRPP, whereas upon binding of PRPP to one subunit, the remaining vacant subunit becomes a high affinity site. The binding data were fit to Equation 1.

$$[\text{mol PRPP bound/mol dimer}] = \frac{n(K_2 S + S^2)}{K_1 K_2 + 2K_2 S + S^2} \qquad (1)$$

where K_1 and K_2 are the dissociation constants for the low and high affinity sites, respectively, n is the number of total binding sites per dimer, and S is the concentration of the free PRPP. The average of fitted binding parameters for these three sets of results gave K_1 = 52 ± 12 μM, K_2 = 1.9 ± 1.4 μM, n = 1.8 ± 0.3 mol PRPP bound/mol of dimer. It is interesting to note that although there is an approximate 25-fold difference between the low and high affinity site, the high affinity site has a dissociation constant nearly identical to that of the wild-type (1.9 vs. 1.3 μM). Also, the nonlinear concave shape for the Lineweaver–Burk plots for either PRPP or IMP as variable substrates also suggested the existence of positive cooperativity in substrate binding (Fig. 5). The wild-type enzyme displayed no such cooperativity (results not shown).

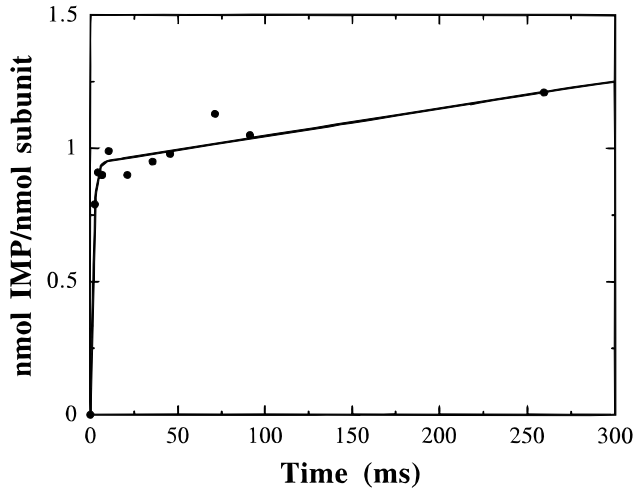

Fig. 4. Pre-steady-state IMP formation by K68A HGPRTase. The line represents the best fit to Equation 2, as described in Materials and methods, using Ultrafit.

The major question that arises is why would changing the residue at position 68 to alanine result in cooperativity between subunits in binding PRPP? Perhaps a partial explanation for this unexpected observation resides in the recently reported structures of a trypanosomal HGPRTase, where the residue homologous with Lys68 was shown to be involved in interactions, which are altered following loop closure as the enzyme approaches the transition state (Focia et al., 1998a). Unfortunately, the side chain of Lys68 in the wild-type human enzyme was disordered, but Eads et al. (1994) predicted that this residue may be involved in binding the pyrophosphate moiety of PRPP when it is present. The structure of the trypanosomal HGPRTase with PRPP in the active site supports this prediction, but the interactions involve main-chain atoms rather than side-chain atoms. In the trypanosomal enzyme, the side chain of Lys68 forms a hydrogen bond with a main-chain atom of a residue in the opposing subunit in the dimer. After closure of the active site, an additional hydrogen bond involving the NZ amine of Lys68 is formed across the dimer interface, and hydrogen bonds between pyrophosphate oxygens and the main-chain nitrogen of Lys68 are lengthened or broken. Thus, the side chain of Lys68 of the trypanosomal HGPRTase is involved in interactions that could influence PRPP binding. The substitution of alanine for lysine at this position would eliminate these interactions between subunits in dimers. Kinetic analyses of the K68A mutant form of the human enzyme support a role for interactions involving Lys68 in suppressing the cooperative binding of PRPP to the second subunit, as well as weakening interactions between pyrophosphate and active site loop containing Lys68 as the enzyme approaches the transition state. Thus, the unexpected appearance of positive cooperativity in the K68A mutant could be a byproduct of interfering with specific interactions that are important for binding PRPP and releasing of pyrophosphate following catalysis in the forward reaction.

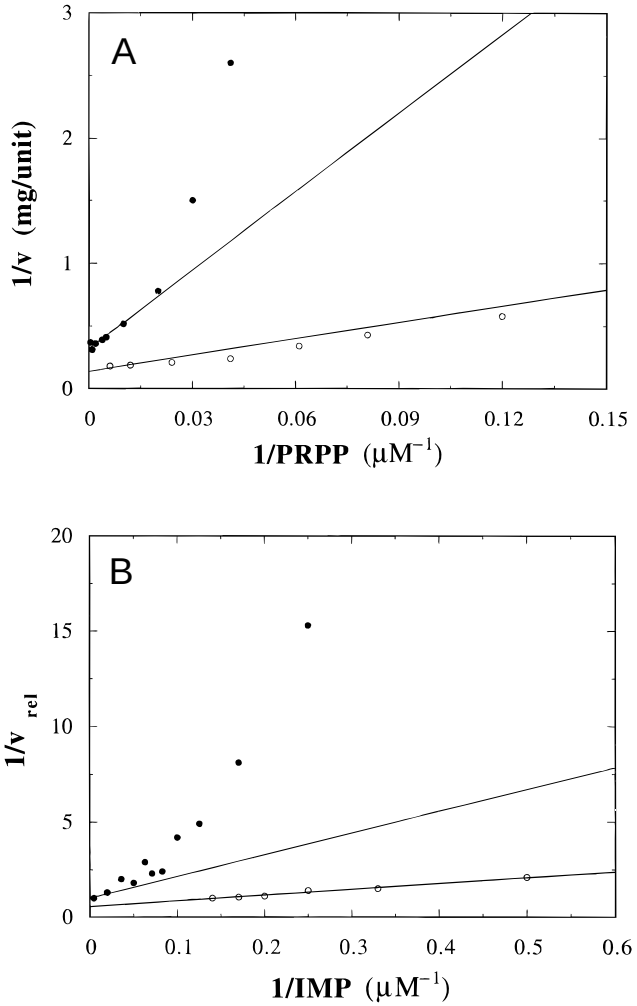

Fig. 5. Lineweaver–Burk plots for (**A**) PRPP and (**B**) IMP as variable substrates. (•) Data sets for K68A. (◦) Data sets for the wild-type taken from Xu et al. (1997). v_{rel} is defined as v/V_{max}. The lines represent the fits using HYPER program of Cleland (1979).

Materials and methods

Site-directed mutagenesis

The K68A mutation was generated following procedures recommended for the BioRad Muta-Gene phagemid in vitro Mutagenesis Kit. A mutagenic oligonucleotide (5′GAATTTATAGCCCCCAGC TAGCACACAGAG) was annealed to the uracil containing single-stranded DNA template, and after second strand synthesis, enrichment for the mutant DNA sequence was achieved using the *E. coli* strain DH5α. For screening purposes, an additional nucleotide substitution was included in the mutagenic oligonucleotide changing the Leu67 codon from CTC to CTA. Together with the change of the Lys68 codon to the one for alanine (AAG to GCT), a unique *Nhe*1 restriction endonuclease recognition site was created. Cloned plasmids containing the diagnostic *Nhe*1 site were sequenced by the dideoxy chain-termination method (Sanger et al., 1977) to confirm the entire sequence of the DNA encoding the human HGPRTase, including the presence of a codon for alanine at position 68.

Recombinant expression and enzyme purification

Five hundred milliliters of low phosphate induction media (Yuan et al., 1990) were inoculated with the Sϕ606 strain of *E. coli* (Δ*pro-gpt-lac, hpt, thi, ara, recA*; refer to Jochimsen et al., 1975) that had been transformed with plasmid (pBAcPRT-68A) encoding the K68A form of the human HGPRTase. Expression was at 37 °C for 20 h (to an A_{600} of over 1.5) in a shaker incubator. Cells were harvested and recombinant enzyme purified as described earlier (Eakin et al., 1997). After elution from GMP–agarose, enzyme buffer exchange was accomplished using a Pharmacia Fast Desalting HR 10/10 FPLC column, enabling removal of trace ions and GMP. Purified enzyme was stored at 4 °C in either TMD buffer (50 mM Tris, pH 7.5, 6 mM $MgCl_2$, 1 mM dithiothreitol—for immediate assay and crystallization studies) or 25 mM ammonium carbonate (for mass spectroscopy). For crystallization studies, the sample was concentrated to 10–15 mg/mL and exchanged into water using an Amicon Centriprep 10 filtration unit. For long-term storage, the enzyme was precipitated with ammonium sulfate at 70% saturation and stored at 4 °C. The precipitate was harvested by centrifugation, and was redissolved in TMD for kinetic studies.

Mass spectrometry

Mass spectrometry was performed at the Duke University Mass Spectrometry Facility using a Micromass VG Quattro BQ triple quadrupole mass spectrometer (Stevens et al., 1994). The mass scale was calibrated with horse heart myoglobin (M_r 16,951.48) with a resolution corresponding to a peak width at a half-height of 1.0 Da for m/z 893. Molecular mass accuracy was of the order of 0.1%. Analysis of the K68A form of the human HGPRTase gave a mass of 24,389.6 ± 1.5 Da, which is consistent with a predicted average mass of 24,391.1 Da.

Crystallization and structure determination

To determine the three-dimensional structure of the human HGPRTase with a purine analog and PRPP bound to the active site, the Ala68 mutant form of the human HGPRTase was cocrystallized with PRPP and HPP (the 9-deaza, 8-aza analog of hypoxanthine). Crystals of the mutant enzyme with HPP and PRPP were obtained using the hanging drop-vapor diffusion method. Three microliters of 10 mg/mL protein solution was mixed with 1 μL of 10 mM HPP, and 10 mM PRPP, 10 mM $MgCl_2$, and 3 μL of precipitant solution containing 100 mM HEPES pH 7.5, 30% PEG 4000. The Mg PRPP HPP complex crystals have unit cell parameters of a = 129.56 Å, b = 65.85 Å, c = 51.46 Å, and $\alpha = \beta = \gamma = 90°$ with the space group of $P2_12_12$. The data set used in this study was collected with a Siemens multiwire area detector equipped with a Rigaku RU-200 rotating anode X-ray source operating at 55 kV and 85 mA, and was reduced using the Siemens package XENGEN (Howard, 1986). The Mg^{2+} PRPP HPP complex data set has an overall R_{sym}, for 9,320 reflections to 2.7 Å resolution (76.2% of the possible data), of 11.7% (on intensities).

For the Mg PRPP HPP complex, the structure of human HGPRTase (Eads et al., 1994) without bound GMP and solvent molecules was used as the starting model. Thirty cycles of rigid body refinement were initially carried out, followed by the simulated annealing procedure "slowcool" described in the X-PLOR manual (Brünger et al., 1990; Brünger, 1992). Both steps were carried out using data between 20.0 and 2.7 Å resolution, applying

a 2σ cutoff. At the end of this first step, the *R*-factor was 24.3%. Cycles of manual rebuilding and refinement were subsequently used to improve the model. The $[(F_o - F_c)\phi_{calc}]$ electron density maps showed interpretable density for PRPP and Mg^{2+} in addition to the peak for HPP in the active site for both the molecules in the asymmetric unit. In addition, density was noticed in the vicinity corresponding to the missing loop residues Leu101 to Gly111 of molecule B, and a few polyalanine residues were built into this extra density. Simulated annealing refinement including these few polyalanine residues for the flexible loop resulted in electron density maps that permitted additional polyalanine residues to be included. This procedure was repeated until polyalanine residues were included for all the residues of the missing loop. Simulated annealing refinement including all the polyalanine residues for the missing loop resulted in electron density maps that enabled the assignment of side-chain atoms for these residues. After the entire flexible loop was modeled in subunit B, the density for the flexible loop in subunit A was improved and allowed tracing the loop in the second monomer as well. In addition, interpretable electron density corresponding to HPP and PRPP moieties was visible for subunit A like subunit B. The residues for the long flexible loop of both the molecules of HGPRTase, Mg^{2+} ions, PRPP, HPP, and 70 water molecules were included in the final refinement. The Mg PRPP HPP complex refined using data between 20.0 and 2.7 Å to a final *R*-factor of 17.4% (R_{free} 27.8) with RMS deviations for bond lengths and bond angles of 0.020 Å and 2.5°, respectively.

Steady-state kinetic studies at 23 °C

Standard spectrophotometric assays were performed, as previously described (Xu et al., 1997), to measure kinetic parameters (k_{cat} and K_m) for K68A HGPRTase-catalyzed IMP formation and IMP pyrophosphorolysis at 23 °C. In all assays, the enzyme was preincubated with appropriate amounts of PRPP (for forward reactions) or IMP (for reverse reactions) followed by addition of the second substrate to initiate the reaction. Values for k_{cat} and K_m were derived with the HYPER program of Cleland (Cleland, 1979) and are reported ± standard errors (Table 1).

Measurement of equilibrium binding

PRPP binding to K68A was determined using equilibrium gel filtration according to earlier procedures (Xu et al., 1997). The range of concentrations used was 1–80 μM for [β-^{32}P]PRPP and 1–40 μM for the HGPRTase subunit.

Rapid quench experiments

Pre-steady-state kinetic experiments were performed at room temperature (22–24 °C) in a Precision Syringe Ram Model 1010 (Update Instrument Inc., Madison, Wisconsin), following the experimental protocols described previously (Xu et al., 1997). A two-syringe setup was employed, one syringe containing PRPP and HGPRTase, and the other [^{3}H]Hx. The final concentrations were 133 μM [^{3}H]Hx, 1 mM PRPP, and 13.1 μM K68A HGPRTase subunits in 100 mM Tris-Cl, 12 mM $MgCl_2$, 5 mM DTT, pH 7.4. The time course of pre-steady-state product formation was fitted to Equation 2 (Johnson, 1995).

$$\frac{\text{mol of IMP formed}}{\text{mol subunit}} = n \times [1 - \exp(-k_{obs}t)] + k_{cat} \times t \qquad (2)$$

where k_{obs} is the first-order rate constant for the rapid phase, and *n* represents the size of the burst of product during the rapid phase.

Supplementary material in Electronic Appendix

Omit map density for the active-site flexible loop in the closed conformation, HPP, and PRPP corresponding to subunit B of the dimer is included in Balendiran.kin file. Electron density calculated with $[(F_o - F_c)\phi_{calc}]$ coefficients and contoured at 1.4σ. The kinemage provided shows electron density maps can be viewed correctly only by the most recent versions of the Mage software. Mage 5.35 or higher is recommended. The most recent version of Mage for the various computer platforms can be obtained from the kinemage ftp server maintained by David and Jane Richardson at Duke University. To obtain the latest version of Mage, connect by anonymous ftp to: kinemage.biochem.duke.edu.

Acknowledgments

We gratefully acknowledge Dr. Charles Grubmeyer for reading the manuscript and making helpful comments. Y.X. and G.K.B. thank Dr. Charles Grubmeyer for his auspices. We thank Félix Rivera for technical contributions and Olivier Froelich (Novartis Produkte AG, Basel, Switzerland) for providing us with HPP. This work was supported in part by the Wolfe-Welch Foundation and NIH Grants AI-34326, GM-52125, AI-38919, and GM-48623. We thank Drs. Jane Richardson and Michael Word for the help on MAGE.

References

Berens RL, Krug EC, Marr JJ. 1995. Purine and pyrimidine metabolism. In: Marr JJ, Müeller M, eds. *Biochemistry and molecular biology of parasites*. New York: Academic Press. pp 89–117.

Bhatia MB, Vinitsky A, Grubmeyer C. 1990. Kinetic mechanism of orotate phosphoribosyltransferase from *Salmonella typhimurium*. *Biochemistry 29*:10480–10487.

Brünger AT. 1992. *X-PLOR version 3.0 manual: A system for crystallographic and NMR*. New Haven, Connecticut: Yale University.

Brünger AT, Krukowski A, Erickson J. 1990. Slow-cooling protocols for crystallographic refinement by simulated annealing. *Acta Crystallogr A46*:585–593.

Cleland WW. 1979. Statistical analysis of enzyme kinetic data. *Methods Enzymol 63*:103–139.

Craig SP III, Focia PJ, Fletterick RJ. 1997. Substitution of lysine for arginine at position 199 of a hypoxanthine phosphoribosyltransferase interferes with binding of the primary substrate to the active site. *Biochim Biophys Acta 1339*:1–3.

Dawson RMC, Elliott DC, Elliott WH, Jones KM. 1986. *Data for biochemical research*, 3rd ed. New York: Oxford University Press. p 408.

Eads JC, Scapin G, Xu Y, Grubmeyer C, Sacchettini JC. 1994. The crystal structure of human hypoxanthine–guanine phosphoribosyltransferase with bound GMP. *Cell 78*:325–334.

Eakin AE, Guerra A, Focia PJ, Torres-Martinez J, Craig SP III. 1997. *Trypanosoma cruzi* as a target for structure-based inhibitor design: Crystallization and inhibition studies with purine analogs. *Antimicrobiol Agents Chemother 41*:1686–1692.

Evans SV. 1993. SETOR: Hardware-lighted three-dimensional solid model representations of macromolecules. *J Mol Graphics 11*:134–138.

Focia PJ, Craig SP III, Eakin AE. 1998a. Approaching the transition state in the crystal structure of a phosphoribosyltransferase. *Biochemistry 37*:17120–17127.

Focia PJ, Craig SP III, Nieves-Alicea R, Fletterick RJ, Eakin AE. 1998b. A 1.4 Å crystal structure for the hypoxanthine phosphoribosyltransferase of *Trypanosoma cruzi*. *Biochemistry 37*:15066–15075.

Giacomello A, Salerno C. 1978. Human hypoxanthine–guanine phosphoribosyl transferase steady state kinetics of the forward and reverse reactions. *J Biol Chem 253*:6038–6044.

Henriksen A, Aghajari N, Jensen KF, Gajhede M. 1996. A flexible loop at the dimer interface is a part of the active site of the adjacent monomer of *Escherichia coli* orotate phosphoribosyltransferase. *Biochemistry 35*:3803–3809.

Hove-Jensen B, Harlow KW, King CJ, Switzer RL. 1986. Phosphoribosylpyrophosphate synthetase of *Escherichia coli*. Properties of the purified enzyme and primary structure of the prs gene. *J Biol Chem 261*:6765–6771.

Howard AJ. 1986. *A guide to data reduction for the Nicolet imaging proportional counter: The XENGEN system*. Gaithersburg, Maryland: Genex Corporation.

Jochimsen B, Nygaard P, Vestergaard T. 1975. Location on the chromosome of *Escherichia coli* of genes governing purine metabolism. Adenosine deaminase (add), guanosine kinase (gsk) and hypoxanthine phosphoribosyltransferase (hpt). *Mol Gen Genet 143*:85–91.

Johnson K. 1995. Rapid quench kinetic analysis of polymerases, adenosinetriphosphatases, and enzyme intermediates. *Methods Enzymol 249*:38–61.

Kelley WN, Greene ML, Rosenbloom FM, Henderson JF, Seegmiller JE. 1969. Hypoxanthine–guanine phosphoribosyltransferase deficiency in gout. *Ann Intern Med 70*:155–206.

Krahn JM, Kim JH, Burns MR, Parry RJ, Zalkin H, Smith JL. 1997. Coupled formation of an amidotransferase interdomain ammonia channel and a phosphoribosyltransferase active site. *Biochemistry 36*:11061–11068.

Kraulis PJ. 1991. MOLSCRIPT: A program to produce both detailed and schematic plots of protein structures. *J Appl Crystallogr 24*:946–950.

Laskowski RA, MacArthur MW, Moss DS, Thornton JM. 1993. PROCHECK: A program to check the stereochemical quality of protein structures. *J Appl Crystallogr 26*:283–291.

Lesch M, Nyhan W. 1964. A familial disorder of uric acid metabolism and central nervous system function. *Am J Med 36*:561–570.

Munagala NR, Chin MS, Wang CC. 1998. Steady-state kinetics of the hypoxanthine–guanine–xanthine phosphoribosyltransferase from *Tritrichomonas foetus*: The role of threonine-47. *Biochemistry 37*:4045–4051.

Musick DL. 1981. Structural features of the phosphoribosyltransferases and their relationship to the human deficiency disorders of purine and pyrimidine metabolism. *CRC Crit Rev Biochem 11*:1–34.

Ozturk DH, Dorfman RH, Scapin G, Sacchettini JC, Grubmeyer C. 1995. Locations and functional roles of conserved lysine residues in *Salmonella typhimurium* orotate phosphoribosyltransferase. *Biochemistry 34*:10755–10763.

Sanger F, Nicklen S, Coulson AR. 1977. DNA sequencing with chain-terminating inhibitors. *Proc Natl Acad Sci USA 74*:5463–5467.

Scapin G, Grubmeyer C, Sacchettini JC. 1994. Crystal structure of orotate phosphoribosyltransferase. *Biochemistry 33*:1287–1294.

Scapin G, Ozturk DH, Grubmeyer C, Sacchettini JC. 1995. The crystal structure of the orotate phosphoribosyltransferase complexed with orotate and alpha-D-5-phosphoribosyl-1-pyrophosphate. *Biochemistry 34*:10744–10754.

Seegmiller JE, Rosenbloom FM, Kelley WN. 1967. Enzyme defect associated with a sex-linked human neurological disorder and excessive purine synthesis. *Science 155*:1682–1684.

Somoza JR, Chin MS, Focia PJ, Wang CC, Fletterick RJ. 1996. Crystal structure of the hypoxanthine–guanine–xanthine phosphoribosyltransferase from the protozoan parasite *Tritrichomonas foetus*. *Biochemistry 35*:7032–7040.

Stevens RD, Bonaventura J, Bonaventura C, Fennel TR, Millington DS. 1994. Application of electrospray ionization mass spectrometry for analysis of haemoglobin adducts with acrylonitrile. *Biochem Soc Trans 22*:545–549.

Strauss M, Behlke J, Ampers F, Goerl M. 1978. Evidence against the existence of real isozymes of hypoxanthine phosphoribosyltransferase. *Eur J Biochem 90*:89–97.

Vos S, de Jersey J, Martin JL. 1997. Crystal structure of *Escherichia coli* xanthine phosphoribosyltransferase. *Biochemistry 36*:4125–4134.

Vos S, Parry RJ, Burns MR, de Jersey J, Martin JL. 1998. Structures of free and complexed forms of *Escherichia coli* xanthine–guanine phosphoribosyltransferase. *J Mol Biol 282*:875–889.

Wilson JM, Young AB, Kelley WN. 1983. Hypoxanthine–guanine phosphoribosyltransferase deficiency. The molecular basis of the clinical syndromes. *N Engl J Med 309*:900–910.

Xu Y, Eads J, Sacchettini JC, Grubmeyer C. 1997. Kinetic mechanism of human hypoxanthine–guanine phosphoribosyltransferase: Rapid phosphoribosyl transfer chemistry. *Biochemistry 36*:3700–3712.

Yuan L, Craig SP III, McKerrow JH, Wang CC. 1990. The hypoxanthine–guanine phosphoribosyltransferase of *Schistosoma mansoni*. Further characterization and gene expression in *Escherichia coli*. *J Biol Chem 165*:13528–13532.

Yuan L, Craig SP III, McKerrow JH, Wang CC. 1992. Steady-state kinetics of the *schistosomal* hypoxanthine–guanine phosphoribosyltransferase. *Biochemistry 31*:806–810.